Type: RESEARCH PAPER
Section: SENSORS AND PHOTONIC DEVICES

## Temperature Sensor based on Optical Fibers with Slanted Ends

# Sensor de Temperatura Soportado en Fibras Ópticas de Extremos Inclinados.

Brayan Patiño-Jurado\*, Luisa Alvarez-Villa, Sebastian Ocampo Gutierrez, Juan F. Botero-Cadavid, Jorge Garcia-Sucerquia.

Universidad Nacional de Colombia Sede Medellín, School of Physics, A.A: 3840-Medellín-050034, Colombia

(\*) E-mail: <a href="mailto:bipatinoj@unal.edu.co">bipatinoj@unal.edu.co</a>

Received: 12/12/2021 Accepted: 31/01/2022 DOI: 10.7149/OPA.55.1.51093

## ABSTRACT:

In this work, a low-cost temperature sensor based on step-index optical fibers with a slanted surface at the distal is fabricated and tested. Distal ends of a series of optical fibers are mechanically polished to obtain slanted surfaces at  $45^{\circ}$ ,  $30^{\circ}$ , and  $22.5^{\circ}$  and are tested in a sensor in the temperature range from  $20^{\circ}$ C to  $220^{\circ}$ C, exhibiting a spectral response to temperature with sensitivities of up to  $21.5^{\circ}$  pm/°C.

Key words: Fiber optics, Slanted end optical fiber, Temperature sensor, Michelson interferometer.

**RESUMEN:** En este trabajo, un sensor de temperatura de bajo costo, soportado en la tecnología de fibras ópticas de salto de índice con extremos inclinados, es fabricado y evaluado. A un conjunto de fibras ópticas se les modifica sus extremos por medio de pulido mecánico con el objetivo de obtener superficies inclinadas a 45°, 30° y 22.5° que pueden evaluarse como sensores de temperatura en el rango de 20° C a 200 ° C. El sensor desarrollado a partir de estas estructuras muestra una respuesta espectral al cambio de temperatura con sensibilidades de hasta 21.5 pm/°C.

**Palabras clave:** Fibra óptica, Fibra óptica de extremo inclinado, Sensor de temperatura, interferómetro de Michelson.

## **REFERENCES AND LINKS / REFERENCIAS Y ENLACES**

- [1] A. Ukil, H. Braendle, and P. Krippner, "Distributed temperature sensing: Review of technology and applications," *IEEE Sensors Journal*, vol. 12, no. 5. pp. 885–892, 2012, doi: 10.1109/JSEN.2011.2162060.
- [2] P. R. N. Childs, J. R. Greenwood, and C. A. Long, "Review of temperature measurement," *Rev. Sci. Instrum.*, vol. 71, no. 8, p. 2959, Jul. 2000, doi: 10.1063/1.1305516.
- [3] A. Ghosh, C. Zhang, S. Q. Shi, and H. Zhang, "High-Temperature Gas Sensors for Harsh Environment Applications: A Review," *CLEAN Soil, Air, Water*, vol. 47, no. 8, p. 1800491, Aug. 2019, doi: 10.1002/CLEN.201800491.
- [4] M. R. Werner and W. R. Fahrner, "Review on materials, microsensors, systems, and devices for high-temperature and harsh-environment applications," *IEEE Trans. Ind. Electron.*, vol. 48, no. 2, pp. 249–257, Apr. 2001, doi: 10.1109/41.915402.
- [5] V. K. Rai, "Temperature sensors and optical sensors," *Appl. Phys. B* 2007 882, vol. 88, no. 2, pp. 297–303, Jul. 2007, doi: 10.1007/S00340-007-2717-4.
- [6] M. Mansoor, I. Haneef, S. Akhtar, A. De Luca, and F. Udrea, "Silicon diode temperature sensors—A review of applications," *Sensors Actuators A Phys.*, vol. 232, pp. 63–74, Aug. 2015, doi: 10.1016/J.SNA.2015.04.022.



- [7] Y. Zhan, H. Wu, Q. Yang, S. Xiang, and H. He, "Fiber grating sensors for high-temperature measurement," *Opt. Lasers Eng.*, vol. 46, no. 4, pp. 349–354, Apr. 2008, doi: 10.1016/J.OPTLASENG.2007.10.008.
- [8] J. Chen, Y. Zhu, Z. Guo, and A. G. Nasibulin, "Recent progress on thermo-electrical properties of conductive polymer composites and their application in temperature sensors," *Eng. Sci.*, vol. 12, pp. 13–22, 2020, doi: 10.30919/ES8D1129.
- [9] N. Sabri, S. A. Aljunid, M. S. Salim, R. B. Ahmad, and R. Kamaruddin, "Toward Optical Sensors: Review and Applications," *J. Phys. Conf. Ser.*, vol. 423, no. 1, p. 012064, Apr. 2013, doi: 10.1088/1742-6596/423/1/012064.
- [10] K. K. K. Annamdas and V. G. M. Annamdas, "Review on developments in fiber optical sensors and applications," *Fiber Opt. Sensors Appl. VII*, vol. 7677, p. 76770R, Apr. 2010, doi: 10.1117/12.849799.
- [11] Y. M. Raji, H. S. Lin, S. A. Ibrahim, M. R. Mokhtar, and Z. Yusoff, "Intensity-modulated abrupt tapered Fiber Mach-Zehnder Interferometer for the simultaneous sensing of temperature and curvature," *Opt. Laser Technol.*, vol. 86, pp. 8–13, Dec. 2016, doi: 10.1016/J.OPTLASTEC.2016.06.006.
- [12] N. Zhao *et al.*, "High Temperature High Sensitivity Multipoint Sensing System Based on Three Cascade Mach–Zehnder Interferometers," *Sensors 2018, Vol. 18, Page 2688*, vol. 18, no. 8, p. 2688, Aug. 2018, doi: 10.3390/S18082688.
- [13] B. H. Lee, E. S. Choi, H. Y. Choi, K. S. Park, S. J. Park, and U.-C. Paek, "Miniature fiber-optic high temperature sensor based on a hybrid structured Fabry–Perot interferometer," *Opt. Lett. Vol. 33, Issue 21, pp. 2455-2457*, vol. 33, no. 21, pp. 2455–2457, Nov. 2008, doi: 10.1364/OL.33.002455.
- [14] T. Wang, K. Liu, J. Jiang, M. Xue, P. Chang, and T. Liu, "A large range temperature sensor based on an angled fiber end," *Opt. Fiber Technol.*, vol. 45, pp. 19–23, Nov. 2018, doi: 10.1016/I.YOFTE.2018.04.008.
- [15] Y. Yu *et al.*, "High-Temperature Sensor Based on 45° Tilted Fiber End Fabricated by Femtosecond Laser," *IEEE Photonics Technol. Lett.*, vol. 28, no. 6, pp. 653–656, Mar. 2016, doi: 10.1109/LPT.2015.2504095.
- [16] Y. Liu, W. Peng, Y. Liang, X. Zhang, X. Zhou, and L. Pan, "Fiber-optic Mach-Zehnder interferometric sensor for high-sensitivity high temperature measurement," *Opt. Commun.*, vol. 300, pp. 194–198, Jul. 2013, doi: 10.1016/J.OPTCOM.2013.02.054.
- [17] C. Liao *et al.*, "Femtosecond laser microprinting of a polymer fiber Bragg grating for highsensitivity temperature measurements," *Opt. Lett. Vol. 43, Issue 14, pp. 3409-3412*, vol. 43, no. 14, pp. 3409–3412, Jul. 2018, doi: 10.1364/OL.43.003409.
- [18] D. Chu, J. Duan, K. Yin, X. Dong, Y. Song, and Z. Xie, "High temperature-sensitivity sensor based on long period fiber grating inscribed with femtosecond laser transversal-scanning method," *Chinese Opt. Lett. Vol. 15, Issue 9, pp. 090602-*, vol. 15, no. 9, pp. 090602-, Sep. 2017, Accessed: Jul. 26, 2021. [Online]. Available: https://www.osapublishing.org/abstract.cfm?uri=col-15-9-090602.
- [19] D. Wu, T. Zhu, and M. Liu, "A high temperature sensor based on a peanut-shape structure Michelson interferometer," *Opt. Commun.*, vol. 285, no. 24, pp. 5085–5088, Nov. 2012, doi: 10.1016/j.optcom.2012.06.091.
- [20] N. Zhao *et al.*, "High temperature probe sensor with high sensitivity based on Michelson interferometer," *Opt. Commun.*, vol. 343, pp. 131–134, May 2015, doi: 10.1016/J.OPTCOM.2014.12.012.
- [21] P. L. Swart, "Long-period grating Michelson refractometric sensor," *Meas. Sci. Technol.*, vol. 15, no. 8, pp. 1576–1580, Jul. 2004, doi: 10.1088/0957-0233/15/8/025.
- [22] L. Bao, X. Dong, P. P. Shum, and C. Shen, "Compact Temperature Sensor with Highly Germania-Doped Fiber-Based Michelson Interferometer," *IEEE Sens. J.*, vol. 18, no. 19, pp. 8017–8021, Oct. 2018, doi: 10.1109/JSEN.2018.2864799.
- [23] J. Yin *et al.*, "Assembly-Free-Based Fiber-Optic Micro-Michelson Interferometer for High Temperature Sensing," *IEEE Photonics Technol. Lett.*, vol. 28, no. 6, pp. 625–628, Mar. 2016, doi: 10.1109/LPT.2015.2503276.
- [24] J. Guo *et al.*, "High-Temperature Measurement of a Fiber Probe Sensor Based on the Michelson Interferometer," *Sensors 2022, Vol. 22, Page 289*, vol. 22, no. 1, p. 289, Dec. 2021, doi: 10.3390/S22010289.



- [25] E. Hecht, *Optics, 4th edition*. 2001.
- [26] H. Gao, Y. Jiang, Y. Cui, L. Zhang, J. Jia, and L. Jiang, "Investigation on the thermo-optic coefficient of silica fiber within a wide temperature range," *J. Light. Technol.*, vol. 36, no. 24, pp. 5881–5886, Dec. 2018, doi: 10.1109/JLT.2018.2875941.
- [27] J. Pascau, "Image Processing with ImageJ | Packt Publishing," no. 1, Accessed: Mar. 21, 2022. [Online]. Available: http://www.packtpub.com/image-processing-with-imagej/book.

## 1. Introduction

The demand for reliable high-temperature sensors has been constant over the last decades in different branches of engineering, such as structure health monitoring of furnaces, turbine engine, nuclear reactors, and electrical transformers, as well as in material processing, and monitoring of exothermic chemical reactions [1,2]. The harsh environments in which the high-temperature measurements takes place demand for compact, resistant, lightweight, cost-effective, and chemically inert sensing technologies besides the ability to operate remotely [3,4]. For this purpose, electrical and optical sensors have found a great interest over the last few decades becoming the de-facto sensors used to measure temperature in industrial applications [5, 6]. Nonetheless, traditional electrical temperature sensors have some disadvantages, including limited sensitivity, low temperature stability, and latent danger of fire accidents [7,8]. In response to these difficulties, temperature sensors based on fiber optics have been widely reported for different applications in recent years thanks mainly to their features such as: their good durability, reliability, biocompatibility, high accuracy, temperature resistance, and electromagnetic interference immunity [9, 10].

Interferometric and fiber grating sensors are the two main kinds of temperature sensors based on fiber optics technology [9,11]. Among the temperature sensors based on interferometers, Mach-Zehnder interferometers (MZIs) [12, 13], Fabry-Perot interferometers (FPIs) [13], and Michelson interferometers (MIs) [11, 15], have been widely investigated in recent years. Temperature sensors based on MZIs have reported sensitivities up to 128.6 pm/°C in the range from 400 °C to 850 °C [16]; FPIs have shown sensitivities up to 173.5 pm/°C in the range from 80°C to 100 °C; and MIs have demonstrated sensitivities to 17.86 pm/°C in the range from 250 °C which increases with the raise of the temperature [14]. Whereas temperature sensors based on fiber grating sensors such as the fiber Bragg gratings [17] and the long period fiber gratings [18], reported sensitivities up to 220 pm/°C and 184.64 pm/°C, correspondingly, for the temperature range from 24 °C to 400 °C [18].

Overall, the interferometric sensors have some advantages over the fiber grating sensors such as the ease of manufacture, low cost, and thermal stability [1, 11]; and besides from their lower sensitivity, MIs have been reported as robust, reliable, and cost-effective structures being the easiest to be manufactured and implemented [9].

To take full advantage of the exceptional features of the temperature interferometric sensors based on fiber optics, in particular the MIs based sensors, such as the cost-effectiveness, easiness of manufacture, thermal stability, reliability, and resistance to high temperature, in this work, angled fibers ends are mechanically polished to experimentally prove the ability to tailor the sensitivity of this sensing structure up to  $21.5 \, \text{pm/°C}$  in the temperature range of 25 to  $220 \, ^{\circ}\text{C}$ . This sensitivity is comparable to that achieved with other sensors based on Michelson interferometers, as reported in [19, 24] but at a fraction of the cost involved in manufacturing them.

## 2. Materials and Methods

## 2.a. Operating Principle

Interferometers based on a slanted surface at the distal end of the fiber at angles of  $45^{\circ}$ ,  $30^{\circ}$ , and  $22.5^{\circ}$ , are illustrated in Fig. 1; for sake of simplicity, only the sagittal plane is represented. A coarse light-ray analysis shows that, based on the Snell's law, when the light propagating in the fiber core impinges on the slanted face of the end of the fiber one total internal reflection (TIR) takes place. After this TIR, the reflected light reaches the interface of the fiber core and the fiber cladding where it splits into two beams at the interface. One beam  $I_1$  is refracted into the cladding towards the cladding/air interface where the light can suffer: one simple retroreflection, panel (a), one total internal refraction, panel (b), or multiple total internal reflections, panel (c). In the same way, the second beam  $I_2$  in the core can suffer from: one simple



retroreflection, panel (a), one total internal refraction, panel (b), or multiple total internal reflections, panel (c) on the core/cladding interface. The refracted wave vectors of  $I_1$  and the reflected wave vector of  $I_2$  are guided along the original path and propagate backwards along with a phase difference  $\Delta \phi$ , superposing and producing an interference at the fiber output whose intensity can be defined by [25]

$$I = I_1 + I_2 + 2\sqrt{I_1 I_2} \cos \Delta \phi. \tag{1}$$

Where  $\Delta\phi=2\pi L/\lambda$ . Here  $L=2n_c l$ , with l the geometric length of the path followed by a beam through the medium of refractive index  $n_c$ , is the optical path difference that can be obtained geometrically for any of the three interferometric structures showed in Fig. 1. Therefore, by tuning the angle of the slanted end of the fiber to 45°, 30°, and 22.5° optical paths differences of 182.6  $\mu$ m, 302.3  $\mu$ m, and 416.7  $\mu$ m can be achieved respectively.

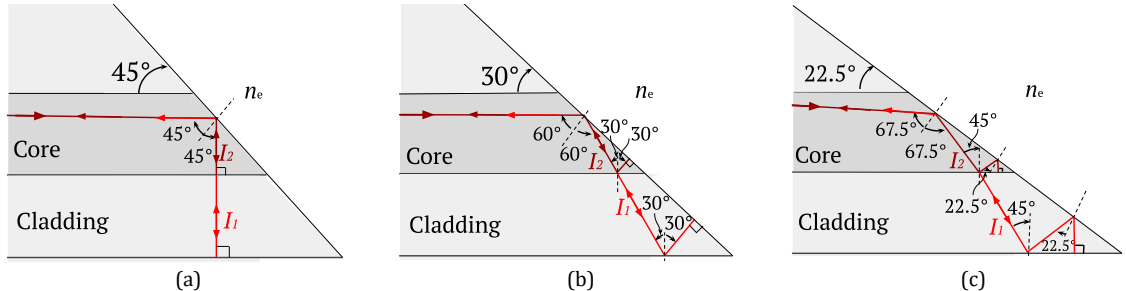


Fig. 1. (Color online). Geometric analysis by ray tracing for three slanted fibers ends with distal end at an angle (a) 45°, (b) 30°, and (c) 22.5°.

In terms of the phase difference, an interference maximum can be obtained when the condition  $\Delta \phi = 2\pi L/\lambda = 2m\pi$ , with m an integer, is fulfilled. Therefore, the corresponding wavelength of the maximum  $\lambda_m$  can be calculated by

$$\lambda_m = \frac{L}{m}.\tag{2}$$

The fringe spacing between two adjacent interference maximums, m = 2 and m = 1, can be expressed as:

$$\Delta \lambda = \frac{\lambda_2 \lambda_1}{L}.\tag{3}$$

Thus, for optical fibers with angle of the slanted end fiber of 45° ( $L=182.6~\mu m$ ), 30° ( $L=302.3~\mu m$ ), and 22.5° ( $L=416.7~\mu m$ ), fringe spacing of 9.7 nm, 5.9 nm, and 4.2 nm can be expected when illumination corresponding at  $\lambda_2 \cong \lambda_1 = 1330~nm$  is used.

Once modeled the optical fiber with their distal end cut at an angle of 45°, 30°, and 22.5° as Mis fiber sensors, in order to use them as a temperature sensor it is needed to analyze the variation of the position of interference maximum in equation (2), with the temperature fluctuation. When the temperature of the slanted fiber end is modified, both refractive index and radius of the fiber are altered because of the thermoptic effect and the thermal expansion of the fiber [26]. Changes of refractive index of the cladding and the geometry of the fiber in turn modify the optical path difference. Thus, the temperature sensitivity of the MI can be derived as [26]:

$$\frac{d\lambda_m}{dT} = \left(\frac{1}{n_{cl}} \cdot \frac{dn_{cl}}{dT} + \frac{1}{r_{cl}} \cdot \frac{dr_{cl}}{dT}\right) \cdot \lambda_m = (\xi + \alpha) \cdot \frac{L}{m}.$$
 (4)

Where  $\xi$  is the thermo-optic coefficient and  $\alpha$  is the thermal expansion coefficient of the optical fiber, for the silica glass fiber  $\xi=1\times 10^{-5}~{\rm K^{-1}}$  and  $\alpha=1\times 10^{-6}~{\rm K^{-1}}$ . These two coefficients are positive, so they both have a positive contribution to the temperature sensitivity in equation (4). As a result, the fluctuation temperature can be monitored by observing the shifting of the maximum, or the minimum, of the wavelength  $\lambda_m$ .



## 2.b. Fabrication of slanted fiber ends and experimental setup.

The fabrication of the slanted fiber ends was done by polishing the distal end on lapping films, as shown in Fig. 2 (a). The slanted fibers ends were fabricated at the end of an optical fiber Corning® SMF28e+ with core/cladding diameter of 8.3/125 µm, using CNC machined hand polish pucks with FC/PC connectors. The polishing pucks were designed so that the end of the optical fiber was sloped, with respect to the lapping film, at angles of 45°, 30°, and 22.5°, respectively. The sensors fabrication process can be completed in two steps: Firstly, three ceramic ferrules with distal ends cut at 45°, 30° and 22.5° were obtained from flat ferrules with 126 μm through-hole. Each FC/PC connector with its ferrule embedded was connected to the slanted polishing puck and placed in contact with a 9 µm diamond lapping film on a slip-free flat working surface. The polishing action took place by gripping this jig with the thumb and forefinger while gently resting it on the polishing lapping moving it with a slight pressure in a figure "8" pattern during five minutes. After obtaining the slanted face on the ferrules, the optical fibers ends were stripped from its polymer jacket and inserted and kept inside the ferrules. A droplet of superglue kept the fibers inside the connectors. For polishing the fiber, 1 µm diamond lapping film was used in a first grinding stage. After grinding the fiber end face with a slight pressure for about 1 min, coarse 45°, 30° and 22.5° angled fibers end faces were completed. To obtain the highest optical properties possible, a second polishing stage using a finer 0.3 µm diamond lapping film and a polishing process of 2 minutes was carried out. Smooth 45°, 30°, and 22.5° angled fibers end faces were obtained, as shown in the pictures of optical microscopy in Fig. 2 (b). The slanted angles were measured on the aforementioned images using the angle tool of the open-source software ImageI [27].

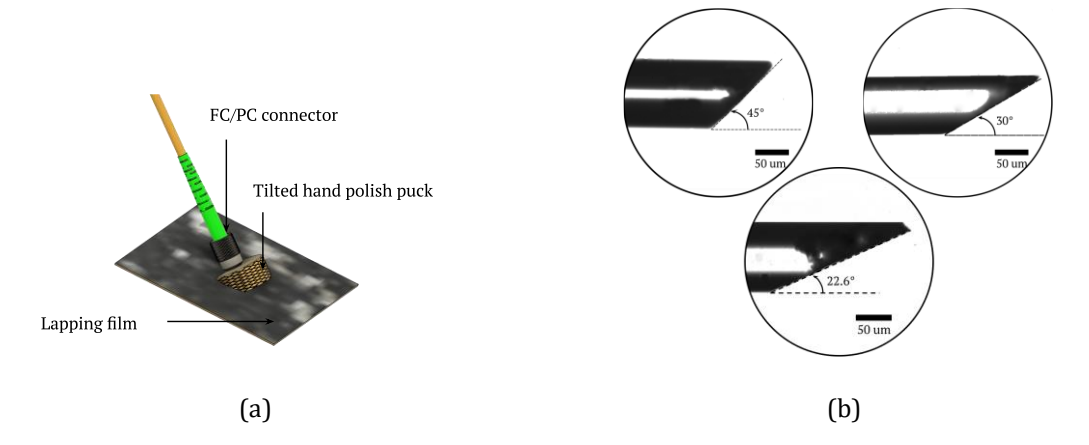


Fig. 2. (Color online). (a) The experimental setup for fabrication of slanted fibers ends by hand polishing using a slanted pucks and lapping films. (b) Optical microscopy images obtained for the optical fibers with their distal end cut at an angle of 45°, 30°, and 22.5°.

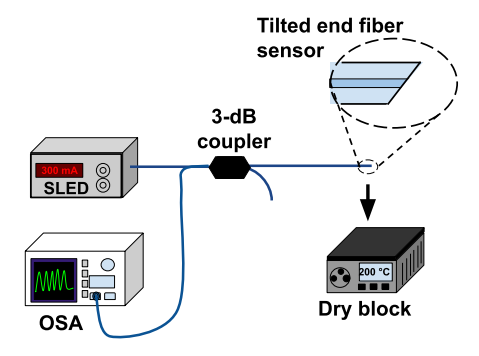


Fig. 3. (Color online). The experimental setup used to test the temperature sensing performance of sensors based on slanted fibers ends.

To study the temperature sensing performance of the fabricated sensors based on slanted fibers ends, a temperature analysis was carried out with the experimental setup shown in Fig. 3. A SLED S5FC1021S (Thorlabs®) with wavelength in the range of 1240 nm to 1405 nm was used as the light source. The interference pattern was measured using an Optical Spectrum Analyzer (OSA) AQ66370D (Yokogawa Electric). The light from the SLED was coupled into each fiber sensor via a directional coupler TW1300R5F2



(Thorlabs®). The light is split into two beams due to the different reflections of the core and cladding at the slanted surface at the distal end of the fiber sensor, the two beams are retroreflected and their wave vectors are superposed in the fiber core again which propagates backwards along causing interference in the output of the fiber which can be observed in the OSA. To study the temperature response of the interferometer pattern, the tip of the optical fiber was placed within a dry block temperature calibrator ETC-400A (Ametek®), which displays an accuracy of  $\pm$  0.5 °C.

## 2.c. Results and discussion.

For each of the three sensors with distal ends cut at 45°, 30°, and 22.5°, the temperature of the dry block calibrator was gradually risen from 25 °C to 220 °C, with 25 °C steps and then cooled down to room temperature with the same pace of 25 °C per step. At every tested temperature point, the reflection spectrum of the sensor was recorded after the temperature have been steady for 10 min to lead to a more accurate measurement. To study the effect of temperature on the interference spectrum recorded by the OSA, one interference peaks on each pattern was taken. For the 45° slanted end at wavelengths near 1313nm; around 1283 nm for the 30°, and around 1315 nm for 22.5° slanted end. As can be observed in the insets of Fig. 4, the fringe spacing between two adjacent interference maxima for each interference pattern were 9.9 nm, 6.5 nm, and 4.1 nm respectively; which is in agreement with the fringe spacing calculated in equation (3). The behavior of the interference patterns for the complete temperature swept, raising the temperature up to 220 °C, is also shown in Fig. 4. A very stable red shift of each pattern occurs with the increase of temperature. To study the sensitivity, a quadratic fitting is used to all data from each temperature response graph. The temperature response curve shows a slight nonlinear nature due to the nonlinearity of thermo-optic effect in a large and high temperature range. The slope of each fit curve was used to calculate the temperature sensitivity, which is found to be a temperature-dependent value in accordance with equation (4). At 200° C, the temperature sensitivities of the fabricated sensors with angle of the slanted end fiber of 45°, 30°, and 22.5° were 10.3 pm/°C, 14.9 pm/°C, and 21.5 pm/°C, respectively.

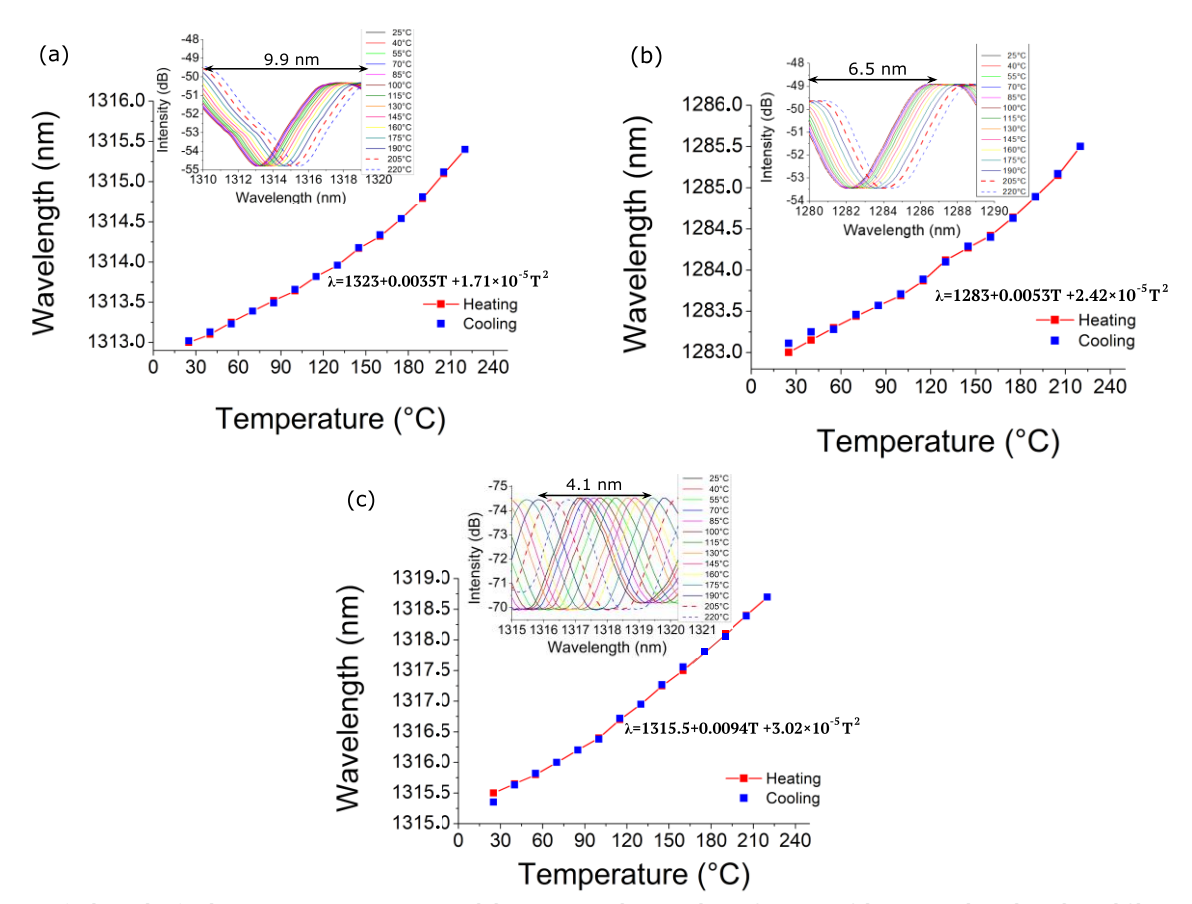


Fig. 4. (Color online). The temperature response, and the corresponding quadratic fit curve, of the sensors based on slanted fibers ends at (a) 45°, (b) 30°, and (c) 22.5°.



In accordance with equation (3), the fringe spacing is inversely proportionate to optical path difference, which is a direct function of the sensitivity. Then, the sensitivity of the temperature sensors based on slanted fiber ends is inversely proportionate to the fringe spacing, as it was experimentally verified according to the results in Fig. 4. The concurrence between the geometrical analysis and the experimentally measured fringe spacing, shows that it is possible to design, model and fabricate with a great degree of confidence temperature sensors based on slanted fibers ends with tailored sensitivities from  $10.3 \text{ pm/}^{\circ}\text{C}$  to  $21.5 \text{ pm/}^{\circ}\text{C}$  in the temperature range of  $25 \text{ to } 220^{\circ}\text{C}$ .

## 3. Conclusions

In this work, the design, fabrication, and testing of a low-cost temperature sensor based on slanted fibers ends were reported. The designed slanted fibers ends were fabricated by mechanical polishing of distal ends of step-index optical fibers to experimentally test the forecasted fringe spacing, by means of regular measurement of interference patterns in an optical spectrum analyzer. The experimental results showed the feasibility of getting sensitivities up to 21.5 pm/°C, in the range of temperature from 25°C to 220°C.

## **Acknowledgements**

This work was supported by Fundación para la Promoción de la Investigación y la Tecnología del Banco de la República de Colombia (Project 4550) and Minciencias, the Ministry of Science, Technology, and Innovation of Colombia (Project 110180763744).

